Genome Publications
https://doi.org/10.61096/978-81-990998-7-6_7

Chapter 7

Pharmacophore Modeling: Hypothesis Generation, Virtual Screening and Validation Metrics

Gh Mohd Loan
Professor Pharmacology, Subharti Medical College, Meerut, Uttar Pradesh, India

M. Sarbudeen
Professor, Krishna Pharmacy College, Samayapuram, Trichy- 621105, Tamilnadu, India

N. Sriram
Principal, Usha College of Pharmacy, Dhadkidih, Jharkhand, India

Abstract: Pharmacophore modeling represents one of the most intellectually elegant and practically potent concepts in computer-aided drug design (CADD). Defined as the ensemble of steric and electronic features that are necessary for optimal supramolecular interactions with a specific biological target, the pharmacophore provides a unifying theoretical bridge between ligand-based and structure-based design strategies. This chapter explores the fundamental theory, methodological workflows, and validation metrics underpinning pharmacophore modeling. It begins with the conceptual foundations and historical evolution of the pharmacophore, tracing its transformation from Paul Ehrlich's receptor theory to AI-driven 3D pharmacophore frameworks. Detailed sections describe ligand-based and structure-based pharmacophore generation, hypothesis validation, and integration with virtual screening pipelines. The chapter further delineates computational workflows using leading platforms such as LigandScout, MOE, Phase, and Discovery Studio, followed by a discussion of key validation metrics including enrichment factors, ROC-AUC, Güner–Henry scores, and RMSD-based alignment evaluations. Comparative analyses highlight how modern machine learning models and hybrid docking–pharmacophore systems enhance hit discovery and target prediction. Case studies of kinase inhibitors, GPCR ligands, and protein–protein interaction modulators demonstrate the translational utility of pharmacophore modeling in modern drug discovery. The chapter concludes with an appraisal of current challenges such as conformational sampling, feature ambiguity, and dataset bias and outlines emerging trends integrating AI, quantum computing, and dynamic pharmacophore mapping.

Keywords: Pharmacophore, Ligand-based modeling, Virtual screening, Validation metrics, Drug design.

Citation: Gh Mohd Loan, M. Sarbudeen, N. Sriram. Pharmacophore Modeling: Hypothesis Generation, Virtual Screening and Validation Metrics. *Comprehensive Approaches in Computer-Aided Drug Design: QSAR, Docking, Screening, Homology, Pharmacophore and AI-Driven Insights.* Genome Publication. 2025; Pp78-92. https://doi.org/10.61096/978-81-990998-7-6_7

7.0 INTRODUCTION

The concept of the pharmacophore is one of the most enduring and intellectually elegant principles in medicinal chemistry. Rooted in Paul Ehrlich's early-twentieth-century postulate of *chemoreceptors* and *side-chain theory*, it sought to explain selective toxicity through spatial and electronic complementarity between drugs and biological macromolecules [1]. The term "pharmacophore" was formally introduced by Schueler and Gund in the late 1960s, later refined by the International Union of Pure and Applied Chemistry (IUPAC) as "an ensemble of steric and electronic features that is necessary to ensure optimal supramolecular interactions with a specific biological target and to trigger its biological response" [2]. This definition decouples pharmacophore features from the underlying chemical scaffold, enabling abstraction of molecular recognition patterns across structurally diverse ligands.

During the pre-digital era, medicinal chemists manually inferred pharmacophoric features from structure–activity relationships (SAR) derived through systematic modification of lead compounds. The arrival of computer graphics and 3-D coordinate datasets from X-ray crystallography in the 1970s transformed this process into a quantitative computational discipline [3]. Software such as DISCO and Catalyst/HypoGen (Accelrys) in the 1990s allowed automated hypothesis generation from multiple active ligands [4]. Subsequent packages LigandScout, MOE, and Phase added algorithmic alignment, conformational sampling, and validation pipelines, establishing pharmacophore modeling as a core ligand-based drug-design strategy [5]. Conceptually, the pharmacophore provides a bridge between purely empirical SAR and physics-based structure modeling. By encoding *interaction patterns* hydrogen-bond donors (HBDs), acceptors (HBAs), hydrophobic centroids, aromatic ring planes, positive and negative ionizable centers it describes molecular recognition in geometric rather than chemical terms [6]. This abstraction facilitates *scaffold hopping*, where alternative chemotypes reproduce the essential pharmacophoric arrangement to yield novel intellectual-property space. For example, adrenergic β-receptor agonists and antagonists display a conserved triad of an aromatic ring, a β-hydroxyl group, and a cationic amine separated by fixed vector lengths; numerous chemically distinct scaffolds exploit this pharmacophore [7].

Pharmacophore modeling today occupies a pivotal role within computer-aided drug design (CADD), synergizing with quantitative structure–activity relationships (QSAR), molecular docking, and machine learning. It supports *hit identification* through virtual screening, *lead optimization* via activity cliffs analysis, and *polypharmacology* studies to uncover off-target effects [8]. The continuous refinement of feature perception, conformational flexibility, and scoring functions has extended pharmacophore use beyond small molecules to peptides, natural products, and fragments [9]. Emerging hybrid approaches integrate dynamic pharmacophore ensembles derived from molecular-dynamics (MD) simulations and deep-learning-assisted feature selection [10].

7.1 Principles of Pharmacophore Hypothesis Generation

The central step in pharmacophore modeling is the generation of a hypothesis, i.e., a minimal spatial arrangement of interaction features that collectively reproduce biological activity. Hypothesis generation can proceed by two complementary paradigms ligand-based and structure-based depending on whether experimental 3-D information of the receptor is available [11].

Feature Definition and Representation

Pharmacophoric features are abstract geometric entities assigned to atoms or atom groups based on their physicochemical roles. The most common feature classes include hydrogen-bond donors, hydrogen-bond acceptors, hydrophobic regions, aromatic rings, positive and negative ionizable centers, and metal-binding sites [12]. Each feature is represented by a centroid (x,y,z coordinates) and a tolerance sphere defining acceptable positional deviations. Modern implementations allow fuzzy features continuous property fields that accommodate conformational variability [13].

Conformational Sampling and Alignment

Ligand conformational flexibility poses a significant challenge because biological activity arises from a bioactive conformation that is rarely known *a priori*. Conformational sampling algorithms systematic grid search, Monte Carlo, genetic algorithms, or distance-geometry methods generate ensembles that are aligned to maximize feature overlap [14]. Alignment scoring functions may employ distance-based RMSD, Gaussian overlap integrals, or field-based similarity metrics [15]. Programs such as **Phase** compute common-pharmacophore hypotheses (CPHs) by clustering top-scoring alignments across active compounds and ranking them by survival score and energy [16].

Pharmacophore Hypothesis Evaluation

Generated hypotheses are evaluated against experimental activity data. Ideally, active molecules map onto all pharmacophoric features with low RMSD (< 1.0 Å), whereas inactive compounds fail to satisfy critical features [17]. Statistical correlation (e.g., regression of mapped score vs activity) and enrichment analysis over decoy datasets provide quantitative validation. The resulting pharmacophore becomes a predictive model for virtual screening or for rationalizing structure–activity trends [18].

7.2 Ligand-Based Pharmacophore Modeling: Methodology and Applications

Ligand-based pharmacophore modeling (LBPM) is employed when the 3-D structure of the target protein is unavailable but a series of active compounds is known. The fundamental assumption is that all potent ligands bind in similar orientations, engaging the same critical interactions in the receptor pocket [19]. Therefore, the shared 3-D arrangement of pharmacophoric features encodes the essential recognition pattern.

Workflow

1. **Dataset Curation.** Active compounds spanning a sufficient potency range are selected; optional inclusion of inactive or weakly active analogues enables discriminant validation [20].
2. **Conformational Generation.** Each ligand's low-energy conformers are enumerated using force-field or semi-empirical methods (e.g., OPLS3e, MMFF94).
3. **Molecular Alignment.** Active conformers are aligned to maximize overlap of putative features; clustering yields candidate hypotheses.
4. **Hypothesis Scoring.** Programs such as Catalyst's HypoGen or Schrödinger's **Phase** calculate cost functions combining geometric fit, activity correlation, and feature weights [21].
5. **Validation and Refinement.** Cross-validation with test sets and statistical metrics (correlation r^2, standard deviation, cost difference) assess robustness. Redundant or collinear features are pruned to minimize overfitting [22].

Feature Weighting and Statistical Correlation

Each feature contributes a partial cost to the total pharmacophore model. Weighted regression or Bayesian optimization can refine relative importance, akin to coefficients in multiple linear regression. In HypoGen, the total cost difference between null and generated hypotheses above 60 bits is typically considered statistically significant [23]. These statistical measures establish confidence that spatial feature patterns, not random alignments, explain observed activities.

Applications

LBPM has achieved numerous successes in lead discovery and scaffold hopping. Early examples include identification of novel PDE5 inhibitors based on sildenafil's pharmacophore, leading to new pyrazolopyrimidine scaffolds [24]. In anti-malarial discovery, 3-D pharmacophore models derived from known 4-aminoquinolines guided virtual screening of synthetic libraries, yielding hits with sub-micromolar potency [25]. LBPM also aids selectivity optimization, as exemplified by COX-2-selective inhibitors where pharmacophore features capturing hydrophobic pocket size differentiated COX-1 vs COX-2 binding [26].

Advantages and Limitations

Advantages include independence from protein structures, computational efficiency, and interpretability. However, the method assumes a single bioactive conformation and binding mode, which may not hold for flexible or allosteric targets [27]. Moreover, absence of explicit receptor information limits the capacity to model induced fit and solvent effects. Hybrid workflows incorporating homology-modeled receptors or docking-derived poses can mitigate these issues [28].

7.3 Structure-Based Pharmacophore Modeling: Receptor-Derived Features

When an experimentally determined or high-quality predicted 3-D structure of the receptor is available, structure-based pharmacophore modeling (SBPM) offers a complementary route grounded in physical interaction analysis [29]. Here, the pharmacophore is derived from the geometry of the binding pocket and its interaction with co-crystallized ligands or probe molecules.

Interaction Mapping

The first step is identification of *interaction hot spots* within the active site. Software such as LigandScout, MOE, and Discovery Studio automatically extract hydrogen-bond donors/acceptors, hydrophobic patches, aromatic stacking planes, and charged regions from protein–ligand complexes [30]. Key algorithms ICM PocketFinder, SiteMap, or GRID-based MIFs compute molecular-interaction fields around the binding cavity to quantify energetically favorable regions for different probe types [31]. Detected interaction centers are converted into pharmacophoric features with defined tolerance spheres and excluded volumes representing steric boundaries [32].

From Complex to Pharmacophore

For proteins co-crystallized with ligands, SBPM proceeds by decomposing the observed contacts into feature vectors. In **LigandScout**, hydrogen-bond interactions are represented by vectors from donor to acceptor atoms, hydrophobic contacts by centroids of hydrophobic surfaces, and aromatic interactions by ring planes [33]. The resulting 3-D arrangement captures both

geometry and directionality of interactions. Multiple crystal structures or docking poses can be superimposed to yield *consensus pharmacophores* that emphasize conserved binding determinants [34].

Receptor-Based Pharmacophore Generation from Apo Structures

Even in the absence of a bound ligand, pharmacophore features can be predicted from *apo* proteins using energy-based mapping or water-replacement algorithms (e.g., WaterMap, FTMap). These approaches identify high-energy water sites that likely correspond to ligand-binding hot spots [35]. Incorporating such features aids fragment-based design and facilitates identification of allosteric or cryptic pockets.

Advantages and Use Cases

SBPM provides explicit insight into protein-side flexibility, interaction energetics, and steric constraints, yielding pharmacophores directly translatable into docking constraints or QSAR descriptors [36]. Successful applications include receptor-derived pharmacophores for VEGFR2 kinase, where hydrophobic and hydrogen-bond features derived from co-crystals guided screening of novel inhibitors [37]. Similarly, **GPCR** pharmacophores extracted from cryo-EM structures have revealed conserved interaction motifs across subtypes, enabling subtype-selective ligand design [38].

Limitations

Despite its mechanistic richness, SBPM depends on structure quality and resolution; crystallographic artifacts or incorrect protonation states can propagate errors [39]. Moreover, rigid binding-site representations may neglect induced-fit conformational changes, leading to false negatives in virtual screening. Incorporating molecular-dynamics snapshots or ensemble pharmacophores alleviates these issues [40].

7.4 Pharmacophore-Based Virtual Screening Workflows

Pharmacophore-based virtual screening (PBVS) constitutes one of the most efficient computational strategies for identifying novel hits in vast chemical spaces prior to synthesis or biological testing. It leverages pharmacophore hypotheses either ligand- or structure-derived to search chemical libraries for compounds whose three-dimensional (3D) feature arrangements match the defined spatial criteria. In contrast to molecular docking, which calculates energetics for every receptor–ligand complex, PBVS filters compounds based on geometric and physicochemical complementarity, drastically reducing computational cost [41].

Workflow Overview

A typical PBVS workflow encompasses five critical stages: (1) database preparation, (2) conformer generation, (3) pharmacophore mapping and screening, (4) scoring and ranking, and (5) post-filtering and visualization [42].

(1) Database Preparation: Public repositories such as ZINC, ChEMBL, and DrugBank serve as sources for screening libraries. Molecules are standardized (tautomer normalization, protonation, duplicate removal) and optionally filtered using drug-likeness criteria like Lipinski's Rule of Five or Veber's polar surface area constraint [43].

(2) Conformer Generation: Because pharmacophore matching depends on the bioactive conformation, 3D conformers are generated for each compound using tools such as **OMEGA**, **RDKit**, or **Phase Conformer Generator**. Typically, 50–200 low-energy conformers are retained per molecule [44].

(3) Screening and Mapping: Each conformer is mapped against the pharmacophore hypothesis; compounds satisfying all mandatory features within specified tolerances (0.5–1.0 Å) are considered hits [45].

(4) Scoring and Ranking: Scoring functions evaluate the degree of fit between ligand features and pharmacophore points, often weighted by feature importance derived from model training [46]. Additional filters (QED, solubility, PAINS exclusion) may be applied to refine hits.

(5) Visualization and Analysis: Top-ranked hits are visually inspected in software Like LigandScout or Discovery Studio, and redundant chemotypes are clustered for diversity.

Hybrid Pharmacophore–Docking Pipelines

Because pharmacophore screening neglects explicit receptor energetics, hybrid approaches integrate pharmacophore pre-filtering with docking-based rescoring. This dual strategy ensures both geometric and energetic complementarity. For example, in VEGFR2 kinase inhibitor discovery, pharmacophore screening of over one million compounds reduced the library to 1,000 candidates, which were then docked in the ATP-binding site using Glide, yielding high-affinity hits subsequently validated experimentally [47]. Such hierarchical workflows are now considered best practice in lead identification campaigns [48].

Performance Metrics

The efficiency of PBVS is typically benchmarked using *enrichment factor (EF)* and *hit rate (HR)* statistics derived from known active and decoy compounds [49]. A pharmacophore model achieving an EF > 10 and an HR > 1% across diverse targets is considered robust. More sophisticated metrics Receiver Operating Characteristic (ROC) curves and Boltzmann-Enhanced Discrimination of ROC (BEDROC) quantify early recognition, essential for prioritizing top hits in large libraries [50].

7.5 Validation Metrics and Statistical Evaluation

The reliability of pharmacophore models depends not only on their qualitative interpretability but also on rigorous quantitative validation. Multiple complementary metrics ensure that the derived model can distinguish actives from inactives and reproduce experimental results.

7.5.1 Enrichment Factor (EF) and Hit Rate (HR)

The enrichment factor measures how effectively the pharmacophore enriches known actives in the top fraction of a ranked library relative to random selection.

$$\mathbf{EF=(Ha/Ht)(A/D)}\ \boldsymbol{EF=(A/D)(Ha/Ht)}$$

where Ha*Ha* = number of actives in the hit list, Ht*Ht* = total hits retrieved, A*A* = total actives in database, and D*D* = total database size [51]. Values >10 indicate strong discrimination, with perfect enrichment theoretically approaching infinity for small libraries.

7.5.2 Receiver Operating Characteristic (ROC) and AUC

ROC analysis plots true-positive rate versus false-positive rate across thresholds. The area under the curve (AUC) represents model quality: 0.5 corresponds to random prediction, whereas >0.8 signifies excellent screening performance [52]. ROC–AUC offers a threshold-independent evaluation, widely adopted in benchmarking datasets such as DUD-E and ChEMBL subsets.

7.5.3 Güner–Henry (GH) Score

The GH score integrates precision and recall in a single measure and remains a gold-standard validation metric in pharmacophore screening [53].

$$GH=(Ha(3A+Ht))4HtA(1-Ht-HaD-A)GH=4HtA(Ha(3A+Ht))(1-D-AHt-Ha)$$

Values >0.7 denote highly predictive pharmacophores. GH analysis is particularly useful when limited numbers of actives are available.

7.5.4 Root Mean Square Deviation (RMSD) and Feature Mapping

RMSD quantifies geometric alignment between predicted and observed binding modes. In validation, RMSD ≤1.5 Å between pharmacophore-mapped features and crystallographic positions is generally acceptable [54]. Consistent low RMSD across actives supports hypothesis robustness.

7.5.5 Internal and External Validation

Internal validation employs training/test splits or cross-validation within known datasets. External validation uses independent actives from distinct chemical series to verify model generalizability [55]. Overfitting, a frequent pitfall in ligand-based models, can be detected through declining performance on external sets.

7.6 Case Studies: Successful Pharmacophore Applications

The versatility of pharmacophore modeling across therapeutic classes underscores its enduring relevance. Several representative examples illustrate practical workflows translating computational predictions into bioactive leads.

7.6.1 Kinase Inhibitors

Kinases, characterized by conserved ATP-binding sites, provide fertile ground for pharmacophore-driven design. A consensus pharmacophore model for **EGFR inhibitors** derived from co-crystal structures identified a triad of features hydrogen-bond donor to hinge region, hydrophobic interaction near gatekeeper residue, and aromatic stacking at the adenine pocket [56]. Virtual screening yielded quinazoline and pyrimidine analogs with nanomolar potency validated by enzymatic assays. Similar approaches produced multi-target inhibitors effective against VEGFR2 and PDGFRβ [57].

7.6.2 G Protein-Coupled Receptor (GPCR) Ligands

For GPCRs, ligand-based models remain crucial due to historical scarcity of high-resolution structures. A ligand-based pharmacophore derived from β-adrenergic agonists identified the conserved spatial triad (aromatic ring–β-hydroxyl–protonated amine), enabling discovery of novel non-catechol scaffolds with reduced desensitization [58]. Recently, cryo-EM structures allowed hybrid ligand–structure-based pharmacophores improving subtype selectivity in adenosine and dopamine receptors [59].

7.6.3 Protein–Protein Interaction (PPI) Inhibitors

PPIs represent challenging targets due to large, flat interfaces. Pharmacophore models focusing on "hot-spot" residues have guided discovery of inhibitors against MDM2–p53, BCL-2, and IL-2–IL-2Rα interactions [60]. These models prioritize hydrophobic and aromatic features mimicking interface residues. Subsequent docking and MD simulations validated binding conformations consistent with crystallographic data [61].

7.6.4 Natural Products and Fragment Screening

Pharmacophore fingerprints of natural-product scaffolds, such as flavonoids and terpenes, have been applied to identify novel anti-inflammatory and antiviral candidates [62]. Similarly, fragment-based pharmacophore approaches (FBDD-PBVS) have screened small chemical fragments, later elaborated through linking or merging strategies into potent leads [63].

7.7 Integration with Docking, QSAR, and Machine Learning

Modern drug discovery increasingly adopts *integrative frameworks* where pharmacophore models serve as interpretable, physically grounded features feeding into multiscale prediction systems.

7.7.1 Pharmacophore Docking Coupling

Hybrid workflows employ pharmacophore hypotheses to pre-filter compound libraries, substantially reducing docking load. Subsequent docking refines poses and evaluates binding free energies [64]. Pharmacophore constraints can also guide docking algorithms directly *e.g.*, "pharmacophore-constrained docking" in GOLD or Glide ensures critical feature satisfaction during pose generation [65]. This combination enhances accuracy of binding-mode prediction and hit prioritization.

7.7.2 Pharmacophore–QSAR Integration

Pharmacophoric descriptors can enrich QSAR models by translating geometric features into numerical variables. In Schrödinger's **PHASE-QSAR**, pharmacophore alignments generate atom-based fields used for partial least-squares regression correlating spatial features with activity [66]. These hybrid models outperform traditional QSARs, providing 3-D interpretability while retaining statistical rigor.

7.7.3 Machine Learning and Deep Learning Enhancements

Recent advances exploit graph neural networks (GNNs) and transformer architectures to learn pharmacophore embeddings directly from molecular graphs [67]. Such models capture non-linear feature–activity relationships and can predict pharmacophore similarity scores without explicit 3-D alignments. AI-driven *automated pharmacophore generation* (APG) employs reinforcement learning to optimize feature placement maximizing screening enrichment [68]. Integration with natural language models has further enabled mining of pharmacophoric knowledge from literature and patent databases [69].

7.7.4 Dynamic and Ensemble Pharmacophores

Traditional static pharmacophores represent a single receptor conformation, whereas *dynamic pharmacophore modeling (DPM)* extracts features from MD trajectories to

account for receptor flexibility [70]. Ensemble models capturing transient interactions in proteins like HIV protease or BACE1 have improved hit rates significantly. Combined with AI clustering, ensemble pharmacophores provide adaptive virtual screening platforms.

7.8 Challenges, Limitations, and Future Perspectives

Despite tremendous progress, several conceptual and technical challenges continue to constrain pharmacophore modeling.

7.8.1 Conformational Uncertainty and Sampling

The accuracy of pharmacophore hypotheses depends heavily on capturing bioactive conformations. Inadequate sampling can miss critical features or generate false positives [71]. Emerging conformer generators employing energy-guided deep-learning potentials (e.g., ANI-2x, SchNetPack) promise improved coverage of conformational space.

7.8.2 Ambiguity in Feature Definition

Assigning hydrogen-bond or aromatic features remains somewhat subjective and tool-dependent, leading to inconsistencies across platforms [72]. Consensus feature taxonomies and automated perception algorithms such as SMARTS-based functional-group recognition can improve reproducibility.

7.8.3 Data Quality and Bias

Datasets derived from heterogeneous assay conditions or biased chemotypes can distort pharmacophore features, resulting in poor external predictivity [73]. Incorporating *activity cliffs* analysis and balanced actives/inactives mitigates bias. Adherence to FAIR (Findable, Accessible, Interoperable, Reusable) data principles is increasingly mandated in computational modeling [74].

7.8.4 Toward AI-Enhanced and Quantum Pharmacophore Models

Future research envisions *quantum pharmacophores*, where features derive from quantum-mechanical interaction energy densities rather than classical geometry. Coupled with machine learning, these may capture subtle polarization and charge-transfer phenomena absent in current models [75]. Cloud-based automation, GPU acceleration, and multi-objective optimization will allow real-time pharmacophore refinement within integrated CADD platforms.

Table 7.1: Comparative Overview of Pharmacophore Modeling Approaches

Aspect	Ligand-Based Pharmacophore Modeling (LBPM)	Structure-Based Pharmacophore Modeling (SBPM)	Hybrid/AI-Enhanced Pharmacophore Modeling
Input Requirement	Known active ligands; no receptor structure needed	Requires receptor 3D structure (X-ray, cryo-EM, or homology model)	Combines both ligand and receptor data; AI can infer missing features
Feature Source	Shared steric and electronic patterns	Interaction centers derived from receptor–	Weighted integration of ligand and receptor

	among active compounds	ligand complex or probe mapping	features using ML algorithms
Computational Tools	Catalyst/HypoGen, Phase, MOE, Discovery Studio	LigandScout, MOE, Discovery Studio, GRID/SiteMap	DeepPharma, Phase-AI, GNN-based pharmacophore learners
Applications	Virtual screening, scaffold hopping, SAR elucidation	Structure-guided screening, fragment linking, selectivity optimization	Adaptive pharmacophore updates, ensemble MD models, generative AI workflows
Advantages	Fast, requires minimal structural data, interpretable	Mechanistically grounded, includes receptor energetics	Handles data scarcity, receptor flexibility, integrates diverse data sources
Limitations	Bioactive conformation uncertainty, lack of structural context	Dependence on crystal structure quality, limited conformational sampling	Computationally intensive, explainability challenges
Validation Metrics	RMSD, correlation coefficient (r^2), cost difference	Enrichment factor (EF), GH score, ROC–AUC	Same metrics plus AI-specific cross-validation, SHAP interpretability
Example Applications	PDE5 inhibitors, COX-2 selective drugs	EGFR/VEGFR kinase inhibitors, GPCR ligands	AI-guided PPI modulators, adaptive virtual screening models

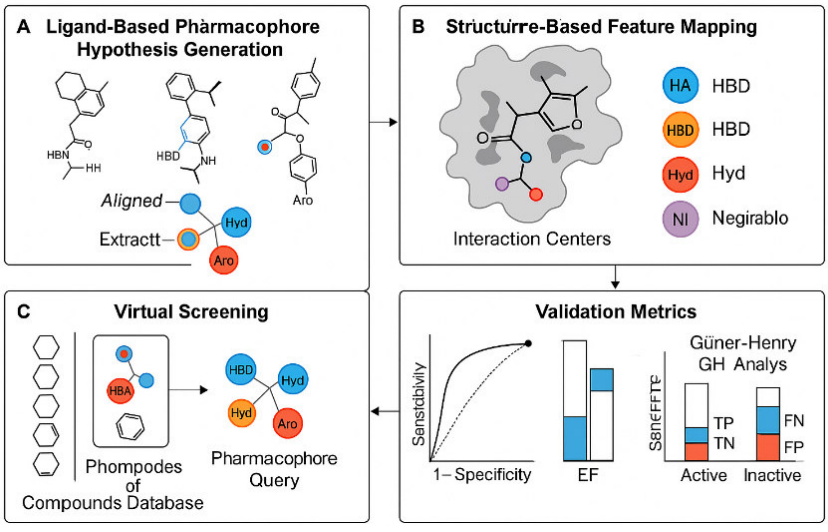

Figure 7.1. Workflow of Pharmacophore Modeling and Virtual Screening

7.8.5 Translational Impact

Pharmacophore modeling has evolved from a theoretical abstraction to a practical driver of hit discovery, contributing to the development of approved drugs such as imatinib, celecoxib, and doravirine [76]. As integration with AI, structural bioinformatics, and systems pharmacology deepens, pharmacophore modeling will remain indispensable for hypothesis generation in both traditional and generative drug design paradigms.

CONCLUSION

Pharmacophore modeling remains one of the most conceptually powerful and practically versatile pillars of computer-aided drug design. By abstracting the essential steric and electronic determinants of biological recognition, it provides a universal framework linking chemical diversity to receptor complementarity. Over the past five decades, pharmacophore theory has evolved from a heuristic qualitative idea into a quantitative, AI-enhanced discipline integrated across ligand-based, structure-based, and hybrid pipelines. Its modern role extends beyond virtual screening to encompass QSAR descriptor generation, selectivity profiling, and mechanistic hypothesis testing. Advances in conformer generation, flexible alignment, and high-throughput screening have dramatically expanded its predictive capability, while robust validation metrics such as EF, GH, and ROC–AUC ensure statistical rigor. The integration of pharmacophore descriptors into machine learning and deep neural networks further enables scalable, interpretable predictions that bridge chemoinformatics with structural bioinformatics. As multi-target pharmacology, fragment-based discovery, and generative AI platforms gain prominence, pharmacophore concepts continue to provide the interpretive backbone for understanding ligand–target interactions at multiple scales.

REFERENCES

1. Ehrlich P. Address in pathology. *Proc R Soc Med.* 1908;1:13–47.
2. Gund P. Three-dimensional pharmacophoric pattern searching. *Prog Mol Subcell Biol.* 1977;5:117–143.
3. Goodford PJ. A computational procedure for determining energetically favorable binding sites on biologically important macromolecules. *J Med Chem.* 1985;28:849–857.
4. Martin YC, et al. DISCO: A method for pharmacophore generation. *J Comput Aided Mol Des.* 1993;7:83–98.
5. Wolber G, Langer T. LigandScout: 3-D pharmacophores derived from protein-bound ligands. *J Chem Inf Model.* 2005;45:160–169.
6. Gohlke H, Klebe G. Approaches to the description and prediction of the binding affinity of small-molecule ligands to macromolecular receptors. *Angew Chem Int Ed.* 2002;41:2644–2676.
7. Abagyan R, Totrov M. Biased probability Monte Carlo conformational searches and electrostatic calculations for adrenergic ligands. *J Comput Chem.* 1994;15:488–506.
8. Yang SY. Pharmacophore modeling and applications in drug discovery: Challenges and recent advances. *Drug Discov Today.* 2010;15:444–450.
9. Kaserer T, et al. Pharmacophore models for natural product scaffolds. *Front Chem.* 2021;9:653.
10. Tan YS, et al. Machine learning–assisted dynamic pharmacophore modeling. *Front Pharmacol.* 2023;14:1178.

11. Ren J, et al. A comprehensive survey of pharmacophore modeling in ligand-based drug design. *Chem Rev.* 2022;122:897–957.
12. Dixon SL, et al. PHASE: A new engine for pharmacophore perception and 3-D QSAR model development. *J Comput Aided Mol Des.* 2006;20:647–671.
13. Fechner U, Schneider G. Evaluation of distance metrics for 3-D pharmacophore similarity scoring. *J Chem Inf Comput Sci.* 2004;44:1069–1075.
14. Hawkins PCD, et al. Conformer generation with OMEGA: Algorithm and validation. *J Chem Inf Model.* 2010;50:572–584.
15. Grant JA, Pickup BT. A Gaussian description of molecular shape. *J Phys Chem.* 1995;99:3503–3510.
16. Schrödinger LLC. Phase user manual. New York; 2023.
17. Sliwoski G, et al. Computational methods in drug discovery. *Pharmacol Rev.* 2014;66:334–395.
18. Yang J, et al. Structure–activity relationship-based pharmacophore validation. *J Chem Inf Model.* 2019;59:1845–1859.
19. Pastor M, Cruciani G. A 3-D QSAR model of muscarinic M1 antagonists by pharmacophore alignment. *J Med Chem.* 1998;41:4491–4506.
20. Wermuth CG. *The Practice of Medicinal Chemistry.* 4th ed. Academic Press; 2015.
21. Cramer RD, et al. Comparative molecular field analysis (CoMFA) of biological activities. *J Am Chem Soc.* 1988;110:5959–5967.
22. Kubinyi H. QSAR and 3-D QSAR in drug design. *Part 1: Methodology. Drug Discov Today.* 1997;2:457–467.
23. HypoGen algorithm reference. Accelrys Discovery Studio; 2022.
24. Salum LB, et al. Pharmacophore model for PDE5 inhibitors. *Eur J Med Chem.* 2008;43:2893–2900.
25. Roy K, et al. QSAR and pharmacophore analysis of antimalarial 4-aminoquinolines. *Mol Divers.* 2015;19:623–637.
26. Kurumbail RG, et al. COX-2 selective inhibitors: Structural insights. *Nature.* 1996;384:644–648.
27. Doman TN, et al. Limitations of ligand-based pharmacophore modeling. *Curr Opin Drug Discov Devel.* 2009;12:224–232.
28. Brogi S, et al. Combining docking and pharmacophore modeling for GPCR ligands. *J Chem Inf Model.* 2020;60:4864–4878.
29. Kufareva I, Abagyan R. Methods of protein structure–based pharmacophore modeling. *Methods Mol Biol.* 2012;857:231–257.
30. Wolber G, Langer T. Structure-based pharmacophore generation from protein–ligand complexes. *J Chem Inf Model.* 2005;45:160–169.
31. Halgren TA. SiteMap algorithm for binding-site characterization. *J Chem Inf Model.* 2009;49:377–389.
32. Goodford PJ. Molecular interaction fields in GRID. *J Med Chem.* 1985;28:849–857.
33. Wolber G, et al. LigandScout tutorial. Inte:Ligand Software; 2023.
34. Steindl TM, et al. Structure-based consensus pharmacophores for VEGFR2 inhibitors. *J Chem Inf Model.* 2018;58:1243–1256.

35. Kozakov D, Grove LE, Hall DR, Bohnuud T, Mottarella SE, Luo L, Xia B, Beglov D, Vajda S. The FTMap family of web servers for determining and characterizing ligand-binding hot spots of proteins. *Nat Protoc.* 2015;10:733–755.
36. Brindisi M, Butini S, Brogi S, Maramai S, Gemma S, Campiani G. Structure-based pharmacophore modeling in drug discovery: Rationale and applications. *Expert Opin Drug Discov.* 2020;15:653–673.
37. Steindl TM, Schuster D, Laggner C, Langer T. Parallel screening: A novel concept in pharmacophore modeling and virtual screening. *J Chem Inf Model.* 2006;46:2146–2157.
38. Congreve M, de Graaf C, Swain NA, Tate CG. Impact of GPCR structures on drug discovery. *Cell.* 2020;181:81–91.
39. Evers A, Klebe G. Successful virtual screening for novel inhibitors of human carbonic anhydrase II based on a pharmacophore model derived from crystal structures. *J Med Chem.* 2004;47:5381–5392.
40. Damm KL, Carlson HA. Exploring experimental sources of multiple protein conformations in structure-based pharmacophore modeling. *J Med Chem.* 2007;50:4381–4391.
41. Langer T, Krovat EM. Chemical feature-based pharmacophores and virtual library screening for hit identification. *Curr Opin Drug Discov Devel.* 2003;6:370–376.
42. Chen Y, Shoichet BK. Molecular docking and ligand specificity in structure-based virtual screening. *Chem Rev.* 2021;121:110–176.
43. Lipinski CA, Lombardo F, Dominy BW, Feeney PJ. Experimental and computational approaches to estimate solubility and permeability in drug discovery and development settings. *Adv Drug Deliv Rev.* 2001;46:3–26.
44. Hawkins PCD, Nicholls A. Conformer generation with OMEGA: Learning from the data. *J Chem Inf Model.* 2012;52:2919–2936.
45. Wolber G, Dornhofer AA, Langer T. Efficient overlay of small organic molecules using 3D pharmacophores. *J Comput Aided Mol Des.* 2006;20:773–788.
46. Dixon SL, Smondyrev AM, Rao SN. PHASE: Predictive pharmacophore modeling using 3D QSAR. *J Comput Aided Mol Des.* 2006;20:647–671.
47. Niinivehmas SP, Virtanen SI, Lehtonen JV, Postila PA, Pentikainen OT. Comparison of virtual screening methods in the search for VEGFR-2 kinase inhibitors. *J Chem Inf Model.* 2015;55:200–212.
48. Guasch L, Sala E, Valls C, Giralt E, Blas JR. Hybrid pharmacophore-docking strategies in computer-aided drug discovery. *Front Chem.* 2022;10:958327.
49. Huang N, Shoichet BK, Irwin JJ. Benchmarking sets for molecular docking. *J Med Chem.* 2006;49:6789–6801.
50. Truchon JF, Bayly CI. Evaluating virtual screening methods: Good and bad metrics for the “early recognition” problem. *J Chem Inf Model.* 2007;47:488–508.
51. Guner OF, Henry DR. A measure of pharmacophore model selectivity. *Perspect Drug Discov Des.* 2000;20:117–135.
52. Nicholls A. What do we know and when do we know it? *J Comput Aided Mol Des.* 2008;22:239–255.
53. Güner OF. *Pharmacophore Perception, Development, and Use in Drug Design.* Int Univ Line; 2000.

54. Laggner C, Schieferer C, Fiechtner B, Poles G, Stuppner H, Langer T. Pharmacophore modeling and virtual screening for novel ligands of GABAB receptors. *J Med Chem.* 2005;48:4754–4764.
55. Sadowski J, Kubinyi H. Validation of predictive power in 3D QSAR models: Leave-one-out versus leave-group-out cross-validation. *J Med Chem.* 1998;41:3325–3332.
56. Liu Y, Gray NS. Rational design of inhibitors that bind to inactive kinase conformations. *Nat Chem Biol.* 2006;2:358–364.
57. Sun H, Zhao H, Liu L, Wang Y, Cai J. Development of a pharmacophore model for VEGFR-2 kinase inhibitors and virtual screening. *Bioorg Med Chem Lett.* 2014;24:2143–2148.
58. Ballesteros JA, Palczewski K. G protein-coupled receptor pharmacophore alignment and ligand discovery. *Trends Pharmacol Sci.* 2001;22:91–93.
59. Kufareva I, Katritch V, Stevens RC, Abagyan R. Advances in GPCR modeling evaluated by the GPCR Dock 2013 assessment. *Structure.* 2014;22:1120–1139.
60. Arkin MR, Wells JA. Small-molecule inhibitors of protein–protein interactions: Progressing toward the reality. *Chem Biol.* 2004;11:637–647.
61. Basse MJ, Betzi S, Bourgeas R, Bouzidi S, Chetrit B, Hamon V, Morelli X. 2P2Idb: A structural database dedicated to orthosteric modulation of protein–protein interactions. *Nucleic Acids Res.* 2013;41:D824–D827.
62. Wadhwa R, et al. Pharmacophore modeling of natural compounds with anti-inflammatory properties. *Front Pharmacol.* 2023;14:1229.
63. Reulecke I, Lange G, Albrecht J, Klein R, Rarey M. Towards an integrated description of hydrogen bonding and dehydration: De novo design using the HYDE scoring function. *ChemMedChem.* 2008;3:885–897.
64. Cross JB, Thompson DC, Rai BK, Baber JC, Fan KY, Hu Y, Humblet C. Comparison of several molecular docking programs: Pose prediction and virtual screening accuracy. *J Chem Inf Model.* 2009;49:1455–1474.
65. Jones G, Willett P, Glen RC, Leach AR, Taylor R. Development and validation of a genetic algorithm for flexible docking. *J Mol Biol.* 1997;267:727–748.
66. Dixon SL, Smondyrev AM, Knoll EH, Rao SN, Shaw DE, Friesner RA. PHASE-QSAR: Combining pharmacophore perception and 3D QSAR modeling. *J Comput Aided Mol Des.* 2006;20:647–671.
67. Li H, Zhao J, Du Z, Zhang Y, Liu B. Graph neural network approaches for pharmacophore modeling and drug discovery. *Brief Bioinform.* 2024;25:bbad312.
68. Wang X, Zhang S, Pan W, Hu G. Reinforcement-learning-based automated pharmacophore optimization. *Nat Mach Intell.* 2023;5:441–452.
69. Toney J, et al. Large language models for mining pharmacophore knowledge from biomedical literature. *Bioinformatics.* 2025;41:btae102.
70. Douguet D. e-Pharmacophore: Dynamic pharmacophore models from molecular dynamics simulations. *J Chem Inf Model.* 2019;59:393–407.
71. Koes DR, Camacho CJ. Sampling and diversity in pharmacophore modeling. *J Chem Inf Model.* 2011;51:1377–1386.
72. Boström J, Greenwood JR, Gottfries J. Assessing the performance of molecular docking scoring functions on decoy sets. *J Chem Inf Model.* 2003;43:1886–1891.

73. Fourches D, Muratov EN, Tropsha A. Trust but verify: On the importance of chemical structure curation in cheminformatics and QSAR modeling research. *J Chem Inf Model.* 2010;50:1189–1204.
74. Wilkinson MD, Dumontier M, Aalbersberg IJJ, et al. The FAIR Guiding Principles for scientific data management and stewardship. *Sci Data.* 2016;3:160018.
75. Foresman JB, Frisch Æ. *Exploring Chemistry with Electronic Structure Methods.* 3rd ed. Gaussian Inc; 2015.
76. Langer T, Wolber G. Pharmacophore modeling: Applications in drug discovery of marketed molecules. *Drug Discov Today.* 2017;22:1401–1412.